J Nanostruct 16(3): 3619-3625, Summer 2026

RESEARCH PAPER

Polyhedral Nickel oxide Nanograin for Ammonia (NH_3) Gas Sensing Applications

Rasha Hamid Ahmed *, Anas Abd Abdullah, N. K. Hassan

Department of Physics, College of Education for Pure Sciences, Tikrit University, Tikrit, Iraq

ARTICLE INFO

Article History:
Received 12 April 2026
Accepted 15 June 2026
Published 01 July 2026

Keywords:
Electrochemical deposition
MSM structure
NH_3 gas sensor
Polyhedral-grained NiO

ABSTRACT

Polyhedral-grained nickel oxide (NiO) nanostructures were electrochemically deposited on silicon Si (111) substrates under a constant deposition time for different applied current density and employed as an active sensing layer for ammonia (NH_3) gas detection. The variation in current density produced polyhedral NiO nanocrystals with different packing densities, which significantly influenced their structural and NH_3 gas-sensing properties. The morphological and structural characteristics of the prepared polyhedral NiO nanocrystals with different densities were investigated using field-emission scanning electron microscopy and X-ray diffraction respectively. A metal–semiconductor–metal (MSM) NH_3 gas sensor with an Al/polyhedral NiO/Al configuration was fabricated using aluminum electrodes. The sensor exhibited promising sensitivity toward ammonia gas, strongly influenced by the size and packing density of the polyhedral NiO grains. Among the prepared samples, the best NH_3 sensing performance was obtained for the NiO sensor fabricated at 3mA/cm^2 applied current density, owing to its well-defined polyhedral grains, high surface coverage, improved crystallinity, and exhibited relatively fast rise and decay times, indicating efficient adsorption and desorption of NH_3 molecules on the NiO surface.

How to cite this article
Hamid Ahmed R., Abd Abdullah A., Hassan N. Polyhedral Nickel oxide Nanograin for Ammonia (NH3) Gas Sensing Applications. J Nanostruct, 2026; 16(3):3619-3625. DOI: 10.22052/JNS.2026.03.052

INTRODUCTION

Nickel Oxide (NiO) had been the subject of many fundamental and applied researches due to its unique an intrinsic p-type semi-conductor material, band gap width of approximately (3.6 to 4 e V) , a good resistivity up to (106 Ω) ,and has ferromagnetic properties with low temperatures and acts as paramagnetic material in high temperatures[1–3].NiO showed a great interest for applications in high-performance and durable electrochemical energy storage systems[4,5],as electrode material for super capacitor applications[6]. NiO is a Promising candidates for the degradation of various organic pollutants due to its photocatalytic activity [7]. In addition NiO has gained significant interest for use in Sensing Applications[8–13].P-type nickel oxide (NiO) semiconductor devices displayed the best photoconductivity gain and sensitivity in photodiodes and dye-sensitized solar cells[14],fast and sensitive ultraviolet photo detector[15],an impressive photo response in the NiO/GO nanocomposite[16]

Various methods have been used to prepare NiO thin layers, including successive ionic layer

* *Corresponding Author Email: rashahamed@tu.edu.iq*

adsorption and reaction (SILAR) method were used to synthesis of hierarchical nanoflake structure of NiO thin film [17], electrochemical deposition [4], atomic layer deposition [16], and pulsed laser deposition [17]NiO thin films synthesized by sol-gel[18]High-quality NiO thin film by spray combustion method at low temperature [19].In reactive sputtering, NiO had been prepared by electron beam evaporation of nickel in an oxygen atmosphere[20]

Electrochemical deposition was adopted as a controllable growth strategy for tailoring polyhedral

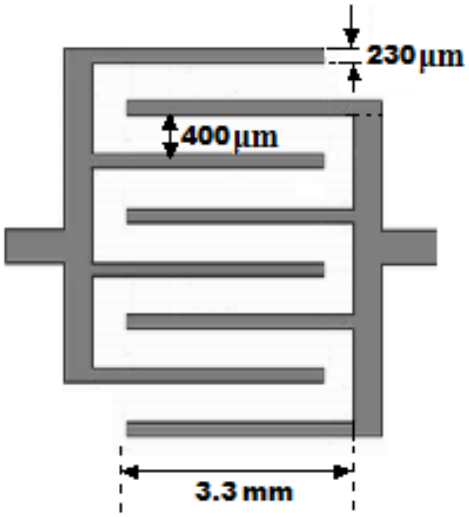

Fig. 1. MSM structure used in the fabrication of MSM Ammonia gas sensor.

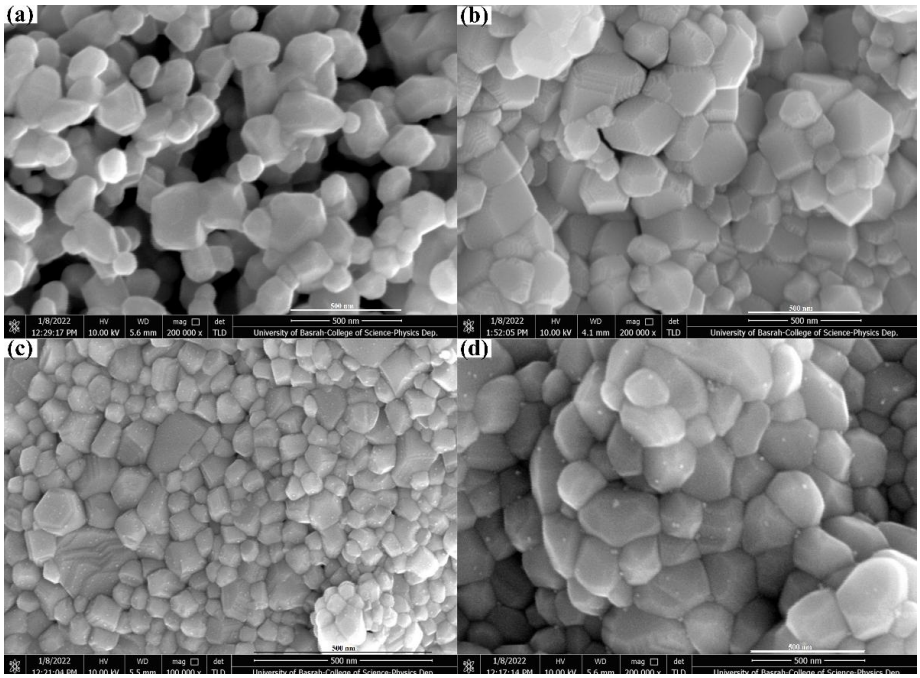

Fig. 2. FESEM images of NiO grown on Si(111) substrate at (a) 1, (b) 2, (c) 3 and (d) 4 mA/cm^2.

NiO nanostructures. In contrast to previous studies that mainly focus on the preparation of NiO thin films, this study demonstrates the role of applied current density as an effective tool for engineering the morphology, grain-boundary network, and sensing activity of polyhedral NiO nanostructures. This approach provides a direct link between electrochemical growth conditions, morphology evolution, and NH_3 gas-sensing behavior, which represents the main novelty of the present work.

MATERIALS AND METHODS

An n-type square pieces with dimensions of 1.3 cm × 1.3 cm, silicon substrates of (111) orientation, (1-10 Ω.cm) as resistivity and thickness about (580 ± 0.25 µm), was used as cathode in electrochemical cell to deposit Ni on silicon substrate. The substrate has been cleaned in isopropanol, methanol and acetone respectively using ultrasonic waves. Native oxide layer removed by immersing the samples were in (HF) solution for 50 sec and then washed with deionized water.

The solution was prepared using nickel chloride ($NiCl_2$) which is a green crystal have molecular weight (23.769 g/mol) to be nickel ions source (Ni^{+2}) in deposition solution. Platinum (Pt) wire was used as anodic electrode. The deposition time was fixed on 120 min., 0.1 M (number of moles) of Sigma-Aldrich Nickel(II) Chloride ($NiCl_2$) as (powder). To obtain a number of moles equivalent to 0.1 M, 1.34 g of $NiCl_2$ powder was dissolved in 50 mL of water.

The deposition current density is an important variable in electrochemical deposition (ECD). We deposited NiO on Si (111) under four deposition current density (1,2,3 and 4 mA/cm^2). At fixed deposition time(120min).). The resulting Ni film was placed inserted in the Oven under ambient environment to oxidize them to produce NiO films. The oven temperature was maintained at 900 °C. The oven temperature was then cooled to room temperature. The morphology produced NiO films were observed with Field Emission Scanning Electron Microscopy (FESEM, NovananoSEM450, FEI). X-ray diffraction (XRD, X'PertPROMPDPANalytical) was used for the structural measurements. NiO nanocrystals NH_3 gas sensor fabricated in vacuum thermal evaporator involves heating a small evaporation boat containing aluminum powder. The contacts are patterned on NiO films by using a metal mask

The change in sensor resistance when exposed to NH_3 gas is taken. The NiO sensor was placed inside the chamber (Fig. 1), later the desired gas (NH_3) with concentration of 78.58 ppm was injected and the Al/polyhedral NiO/Al sensor inside a gas-sensing chamber at two separate operating temperatures 100 °C and 200 °C.

RESULTS AND DISCUSSION

The FE-SEM micrographs in Fig. 2 illustrates the evolution of the NiO surface morphology

Table 1. Crystallite size of NiO nanoparticles using XRD at the dominant diffraction peakNiO (111).

Sample	2θ (°)	FWHM β (rad)	d-spacing (Å)	Lattice parameter a (Å)	Crystallite size D (nm)
NiO-a	37.2	0.0108	2.415	4.183	13.5
NiO-b	37.2	0.0087	2.415	4.183	16.8
NiO-c	37.2	0.0052	2.415	4.183	27.9
NiO-d	37.2	0.00698	2.41	4.183	21.0

Table 2. Crystallite size of NiO nanoparticles using XRD at the dominant diffraction peakNiO (200).

Sample	2θ (°)	FWHM β (rad)	d-spacing (Å)	Lattice parameter a (Å)	Crystallite size D (nm)
NiO-a	43.2	0.01012	2.092	4.185	14.7
NiO-b	43.2	0.00838	2.092	4.185	17.8
NiO-c	43.2	0.00524	2.092	4.185	28.5
NiO-d	43.2	0.00733	2.092	4.185	20.3

as a function of applied current density. The FE-SEM images demonstrate that the applied current density has a pronounced influence on the surface morphology in tailoring the density and arrangement of polyhedral NiO nanograins.

At (1 mA/cm^2) low current density, the deposited layer of NiO shows limited nucleation, the grains appear less dense and randomly distributed, leading to isolated and non-uniformly distributed grains on the Si (111) surface. With increasing current density (2 mA/cm^2), the nucleation density increases significantly, promotes the formation of closely packed polyhedral nanograins. This morphology provides a high density of grain boundaries and surface-active sites, which are essential for gas adsorption and resistance modulation during NH_3 exposure. The enhanced supply of Ni ions and faster electrochemical reaction rate near the substrate surface as a result of changing the applied current density which controls the rate of Ni^{2+} ion reduction and the subsequent nucleation and promotes the formation of a higher number of NiO nuclei, optimum current density (3 mA/cm^2) characterized by dense polyhedral grains and well-developed grain boundaries, produces the best balance between high grain density, surface uniformity, and accessible active sites,

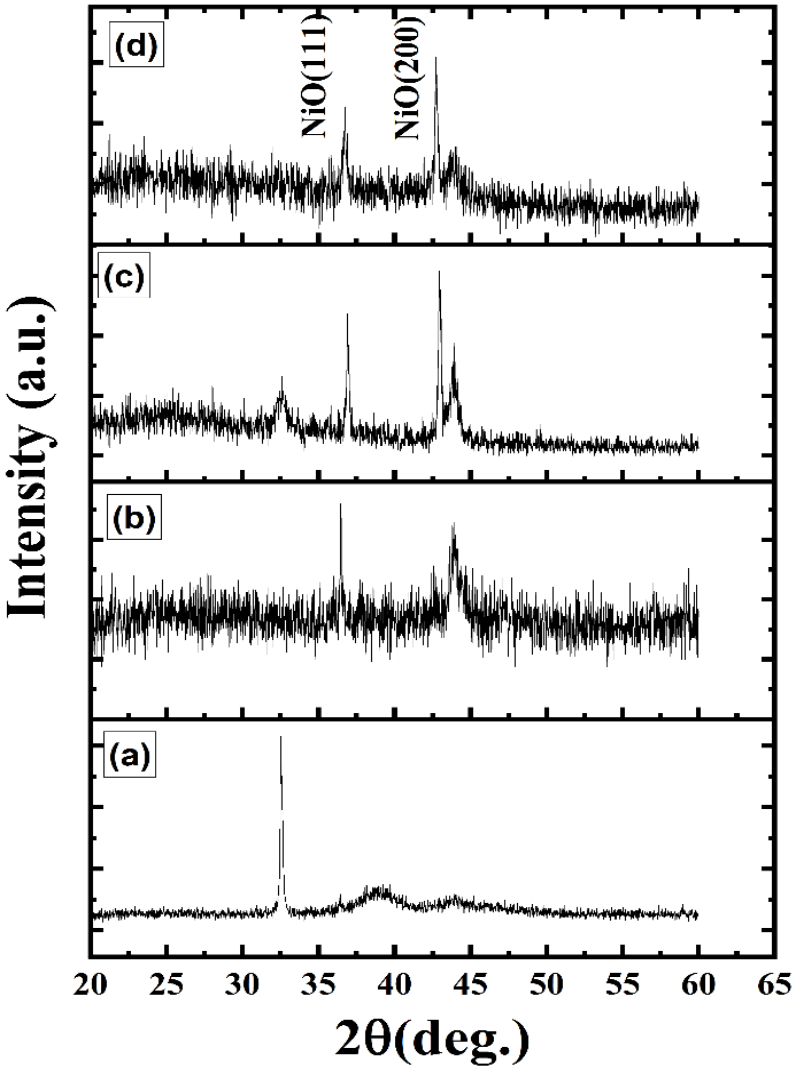

Fig. 3. The XRD patterns of NiO grown on Si(111) substrate at (a) 1, (b) 2, (c) 3 and (d) 4mA/cm^2.

whereas excessive current density may promote overgrowth and grain agglomeration. This current-density-controlled morphology evolution represents an important feature of the present work and directly supports the improved NH_3 gas-sensing performance of the fabricated NiO sensor. However, further increase in current density (4 mA/cm^2) may enhance nucleation and surface coverage, lead to the formation of overly compact and agglomerated polyhedral NiO grains, which can reduce the effective sensing surface. As a result, NH_3 adsorption and surface reaction become less efficient, leading to a lower sensing response.

Fig. 3 presents the XRD patterns of polyhedral NiO nanostructures deposited on Si (111) substrates at different applied current densities. The diffraction peaks located at approximately 2θ = 37° and 43° correspond to the (111) and (200) planes of cubic NiO, respectively, confirming the formation of the face-centered cubic NiO phase. At lower current density (1 mA/cm^2), weak NiO-related peaks with a broad background; one sharp substrate-related peak is visible, indicating smaller crystallite size and lower crystallinity. With increasing current density (2 mA/cm^2), NiO peaks become more visible, especially around 37° and 43° the peaks become sharper and more intense (Fig. 3b), suggesting improved crystallinity and enhanced NiO crystal growth. The dominant (111) peak indicates preferential orientation along the (111) plane. Strong and sharp NiO diffraction peaks; clear peaks at 2θ ≈ 37° and 43° with increasing applied current density to (3 mA/cm^2) (Fig. 3c), the peaks become sharper and more intense, suggesting improved crystallinity and enhanced NiO crystal growth which indicates that the crystallinity of the polyhedral NiO nanostructures is strongly dependent on the electrochemical growth conditions.

NiO peaks are still present but less intense/broader than sample (Fig. 3c) with further increasing the applied current density (4 mA/cm^2) (Fig. 3d), can promote overgrowth and agglomeration of the polyhedral NiO grains, resulting in a more compact structure with fewer accessible active sites for NH_3 adsorption. Therefore, an optimum current density is required to balance crystallinity, surface coverage, and gas-sensing performance. These results demonstrate that the applied current density plays a crucial role in controlling the structural quality of the

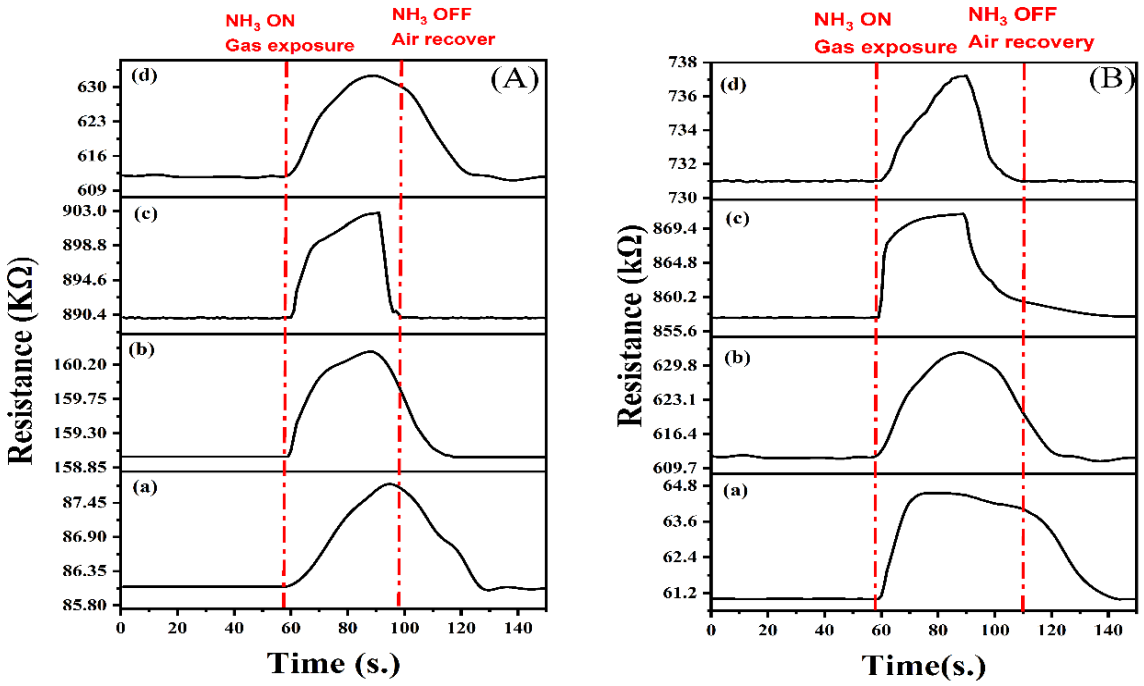

Fig. 4. The Sensitivity of the (Al- NiO -Al) gas sensor measured under 78.8 ppm NH_3 gas flow. (A) Operating temperature at 100 °C (B) Operating temperature at 200 °C.

polyhedral NiO nanostructures. The observed diffraction peaks are consistent with the standard NiO data (JCPDS No. 04-0835) [21–24].

The XRD characteristics of the polyhedral NiO nanostructures deposited at different applied current densities are summarized in Tables 1 and 2. The peak position, FWHM, d-spacing, lattice parameter, crystallite size, were estimated by using Scherrer formula [25]at the dominant NiO diffraction peaksNiO (111).

$$D = \frac{K\lambda}{\beta\cos\theta} \quad (1)$$

The variation in these parameters confirms that the applied current density significantly influences the crystallinity and structural quality of the electrochemically deposited NiO nanostructures.

Sensor response at at 100 °C and 200 °C operating temperatures for 78.58 ppm NH_3 Fig. 4. The sensing response is strongly affected by the density and packing of the polyhedral NiO grains**.** In both cases, the resistance increases upon NH_3 exposure and in air, oxygen molecules are adsorbed on the NiO surface and extract electrons, which increases the hole concentration and decreases the resistance during air recovery, confirming the p-type semiconducting behavior of NiO toward reducing ammonia gas. At 100 °C, the sensor with denser polyhedral NiO grains exhibits a stronger response, indicating that the grain-boundary-rich morphology provides more active sites for NH_3 adsorption. At 200 °C, the response of some samples becomes faster and more pronounced due to enhanced surface reaction kinetics. However, further improvement is not observed for all samples, suggesting that excessive grain compactness or rapid NH_3 desorption may limit the effective gas–surface interaction. Therefore, the sensing performance depends not only on the operating temperature but also on the current-density-controlled morphology of the polyhedral NiO nanostructures.

Operating temperature at 200 °C gives better response (Fig. 4a), indicating improved NH_3 adsorption/reaction kinetics, as can be observed from the behavior of the response curves resistance increases slowly after NH_3 exposure and recovers after air introduction. A clear increase in resistance under NH_3, followed by recovery in air as clearly demonstrated by the response curves in Fig. 4b. shows a much stronger resistance increase and good recovery as its illustrated, the sensing performance at 200 °C, showing a faster response and more efficient recovery compared with the behavior observed at 100 °C. Fig. 4c. shows that 100 °C operating temperature may be more stable, while 200 °C gives stronger gas interaction but slower recovery. Fig. 4d. shows that 100 °C operating temperature is better, while 200 °C may reduce effective sensing due to compact/ agglomerated morphology or fewer accessible sites.Therefore, the different responses observed at 100 °C and 200 °C reflect the combined influence of temperature, surface adsorption/ desorption processes, and current-density-controlled polyhedral morphology. The following tables summarizes the estimated Response and Recovery time s extracted from the response–recovery curves at 100 °C and 200 °C.

The response and recovery times estimated from the dynamic sensing curves are summarized

Table 3. Values of the density and arrangement of polyhedral NiO nanograins-dependent responses of Al- NiO -Al at 100 °C operating temperature.

Temp. (100 °C)	a	b	c	d
Response time (s)	32	26	25	38
Recovery time (s)	22	18	4	24

Table 4. Values of the density and arrangement of polyhedral NiO nanograins-dependent responses of Al- NiO -Al at 200 °C operating temperature.

Temp. (200 °C)	a	b	c	d
Response time (s)	12	24	8	28
Recovery time (s)	30	15	35	12

in Tables 3 and 4. Polyhedral NiO sample (c) exhibited the most balanced NH_3 sensing behavior, showing a fast response at 200 °C and rapid recovery at 100 °C. Therefore, polyhedral NiO nanostructures grown at 3mA/cm^2 represents the optimum sensing layer, where the balance between active surface sites, gas diffusion pathways, grain-boundary network, crystallinity, and charge-transfer efficiency leads to enhanced ammonia sensing behavior.

CONCLUSION

Polyhedral NiO nanostructures were successfully deposited on Si (111) substrates by simply controlling the applied current density during electrochemical deposition (ECD), which was found to play a decisive role in controlling the grain size, packing density, surface coverage, and crystallinity of the sensing layer. and the applied current density Among the prepared samples, NiO nanostructures grown at 3 mA/cm^2 exhibited the optimum performance due to its well-defined polyhedral morphology, improved XRD crystallinity, abundant grain boundaries, and balanced response–recovery behavior toward NH_3 gas. The enhanced performance is attributed to p-type semiconducting nature of NiO, which promote NH_3 adsorption and also to the well-defined polyhedral grains which provided abundant grain boundaries and active surface sites. These findings confirm that current-density-controlled electrochemical deposition is a practical strategy for developing high-performance NiO-based ammonia gas sensors.

CONFLICT OF INTEREST

The authors declare that there is no conflict of interests regarding the publication of this manuscript.

REFERENCES

1. Wawrzyniak J. Advancements in Improving Selectivity of Metal Oxide Semiconductor Gas Sensors Opening New Perspectives for Their Application in Food Industry. Sensors. 2023;23(23):9548.
2. Li P, Wang M, Duan X, Zheng L, Cheng X, Zhang Y, et al. Boosting oxygen evolution of single-atomic ruthenium through electronic coupling with cobalt-iron layered double hydroxides. Nature Communications. 2019;10(1).
3. Ghalmi Y, Habelhames F, Sayah A, Bahloul A, Nessark B, Shalabi M, et al. Capacitance performance of NiO thin films synthesized by direct and pulse potentiostatic methods. Ionics. 2019;25(12):6025-6033.
4. Murugadoss G, Kandhasamy N, Zaporotskova IV, Venkatesh N, Salla S, Pandurengan S. Morphology-controlled nickel oxide nanostructures: unlocking high-performance supercapacitor applications. Chemical Physics Impact. 2025;10:100888.
5. Lesbayev B, Auyelkhankyzy M, Ustayeva G, Yeleuov M, Rakhymzhan N, Maral Y, et al. Modification of Biomass-Derived Nanoporous Carbon with Nickel Oxide Nanoparticles for Supercapacitor Application. Journal of Composites Science. 2023;7(1):20.
6. Lamba P, Singh P, Singh P, Kumar A, Singh P, Bharti, et al. Bioinspired synthesis of nickel oxide nanoparticles as electrode material for supercapacitor applications. Ionics. 2021;27(12):5263-5276.
7. . International Journal of Advanced Biological and Biomedical Research. 2015;4(4).
8. Leprince-Wang Y, Wang GY, Zhang XZ, Yu DP. Study on the microstructure and growth mechanism of electrochemical deposited ZnO nanowires. J Cryst Growth. 2006;287(1):89-93.
9. Gupta A, Kim HW, Kim SS, Mirzai A, Dwivedy SK, Jha RK. Recent progress in nickel oxide-based chemiresistive toxic-gas sensors. Nanoscale. 2025;17(40):23247-23272.
10. Kaur N. Nickel Oxide Nanostructures for Gas Sensing: Recent Advances, Challenges, and Future Perspectives. ACS Sensors. 2025;10(3):1641-1674.
11. Ben Arbia M, Comini E. Growth Processing and Strategies: A Way to Improve the Gas Sensing Performance of Nickel Oxide-Based Devices. Chemosensors. 2024;12(3):45.
12. Kulkarni AA, Shinde SD, Patil GE, Hiremath P, Naik N, Jain GH, et al. Preparation of nickel oxide nanostructure by hydrothermal method as H2S gas sensor. Journal of Materials Science: Materials in Electronics. 2025;36(10).
13. Shailja, Singh KJ, Singh RC. Enhanced toluene sensing performance of nanostructured aluminium-doped nickel oxide gas sensor. Appl Phys A. 2023;129(4).
14. Tsay C-Y, Chen Y-C, Tsai H-M, Lu F-H. Photoresponse of solution-processed transparent heterojunction ultraviolet photodetectors composed of n-type ZTO and p-type NiO-based semiconductor thin films. Materials Chemistry and Physics. 2023;295:127143.
15. Khun K, Ibupoto ZH, Willander M. Development of fast and sensitive ultraviolet photodetector using p-type NiO/n-type TiO_2 heterostructures. physica status solidi (a). 2013;210(12):2720-2724.
16. Walleni C, Hamdaoui N, Fadil D, Nsib MF, Llobet E. Synthesis and characterization of nickel oxide nanoparticles decorated graphene oxide for fast-response UV photodetector: unveiling of negative photoconductance. Journal of Materials Science: Materials in Electronics. 2024;35(18).
17. Gund GS, Lokhande CD, Park HS. Controlled synthesis of hierarchical nanoflake structure of NiO thin film for supercapacitor application. J Alloys Compd. 2018;741:549-556.
18. Jlassi M, Sta I, Hajji M, Ezzaouia H. NiO thin films synthesized by sol-gel: Potentiality for the realization of antireflection layer for silicon based solar cell applications. Surfaces and Interfaces. 2017;6:218-222.
19. Qin Y, Song J, Qiu Q, Liu Y, Zhao Y, Zhu L, et al. High-quality NiO thin film by low-temperature spray combustion method for perovskite solar cells. J Alloys Compd. 2019;810:151970.
20. Rossi CE, Paul W. The preparation of NiO thin films and their use in optical measurements in the visible and ultraviolet. Journal of Physics and Chemistry of Solids. 1969;30(9):2295-2305.
21. Qiao H, Wei Z, Yang H, Zhu L, Yan X. Preparation and Characterization of NiO Nanoparticles by Anodic Arc Plasma Method. Journal of Nanomaterials. 2009;2009(1).
22. Br S, Xr J. Effect of Calcination Time on Structural, Optical and Antimicrobial Properties of Nickel Oxide Nanoparticles. Journal of Theoretical and Computational Science. 2016;03(02).
23. Anand GT, Nithiyavathi R, Ramesh R, John Sundaram S, Kaviyarasu K. Structural and optical properties of nickel oxide nanoparticles: Investigation of antimicrobial applications. Surfaces and Interfaces. 2020;18:100460.
24. Chopade SC, Kore IG, Patil SP, Jadhav ND, Srinidhi C, Desai PA. Lattice geometry controlled synthesis of Cu – Doped nickel oxide nanoparticles. Ceram Int. 2018;44(5):5621-5628.
25. Uddin MJ, Yeasmin MS, Muzahid AA, Rahman MM, Rana GMM, Chowdhury TA, et al. Morphostructural studies of pure and mixed metal oxide nanoparticles of Cu with Ni and Zn. Heliyon. 2024;10(9):e30544.